J Physiol (2003), **549.1**, *pp.* 107–120

DOI: 10.1113/jphysiol.2002.038646
www.jphysiol.org

Journal of Physiology

Functional identification of ion binding sites at the internal end of the pore in *Shaker* K^+ channels

Jill Thompson and Ted Begenisich

Department of Pharmacology and Physiology, University of Rochester Medical Center, Rochester, NY 14642 USA

The inner end of the pore in voltage-gated K^+ channels is the site of conformational changes related to gating and contains binding sites for permeant ions and pore-blocking molecules including quaternary ammonium ions and drugs. In order to determine the location and affinity of ion binding sites we probed the *Shaker* K^+ channel with the quaternary ammonium analogue, tetrabutyl antimony (TBSb), a compound that is sufficiently electron dense to have been observed to occupy the cavity site in the bacterial K^+ channel, KcsA. TBSb has K^+ channel blocking properties analogous to those of tetrabutyl ammonium (TBA), and kinetics slow enough to be reliably measured. In the presence of external TEA, the internal TBSb on-rate decreased with increased internal K^+ concentration as if these permeant ions prevented TBSb access to its site in the pore. The TBSb off-rate in low K^+ was increased with external TEA addition and then reduced with increased internal K^+. We found several differences between the behaviour of internal TBSb and TEA suggesting these molecules bind to distinct but interacting sites in the pore. We also found several differences in how K^+ and Rb^+ ions occupy sites in the inner end of the pore. These data suggest the presence of three sites in the inner end of the pore: (1) a site near the cytoplasmic end that binds TEA and K^+ (but not Rb^+) ions; K^+ ions binding to this site inhibit TBSb exit from the pore; (2) a TBSb site slightly more into the pore that is rarely occupied by K^+ or Rb^+ ions; (3) a site further into the pore that has a high affinity for K^+ and Rb^+ ions; occupancy of this site by these permeant ions increases the TBSb off-rate. These results provide information on the fine-structure of ion interactions with the inner end of the pore in K^+ channels.

(Received 27 December 2002; accepted after revision 28 February 2003; first published online 28 March 2003)
Corresponding author T. Begenisich: Department of Pharmacology and Physiology Box 711, University of Rochester Medical Center, Rochester, NY 14642, USA. Email: ted_begenisich@urmc.rochester.edu

Membrane voltage causes a conformational change in the structure of voltage-gated K^+ channels that opens the ion permeation pathway. This opening occurs at the inner end of the channel and reveals binding sites for quaternary ammonium ions and, in inactivating K^+ channels, a site for the inactivation particle (reviewed in Yellen, 1998). Permeant ions interfere with these gating processes (Armstrong, 1971; Choi *et al.* 1991; Lui *et al.* 1997; Holmgren *et al.* 1997; Melishchuk & Armstrong, 2001). Quaternary ammonium ions, particularly TEA and its analogues, have been valuable tools for probing the functional structure of the inner end of K^+ channel pores (e.g. Armstrong, 1969, 1971; Yellen *et al.* 1991; del Camino *et al.* 2000; Zhou *et al.* 2001*b*; Guo & Lu, 2001; Melishchuk & Armstrong, 2001). The inner part of the pore forms the binding sites for these ions (Yellen *et al.* 1991; del Camino *et al.* 2000) and other open-channel blocking compounds, including agents that induce the potentially fatal cardiac long QT syndrome (Mitcheson *et al.* 2000), bind in the inner end of the pores in K^+ channels.

The bacterial channel KcsA currently serves as model for the structure of the pore in K^+ channels and contains a large, 8 Å (0.8 nm) diameter, water-filled cavity located approximately halfway across the membrane, and a 12 Å-long selectivity filter located on the extracellular side of the pore (Doyle *et al.* 1998; Zhou *et al.* 2001*a*). While the KcsA structure is likely to represent a good model for the extracellular end of the pore in eukaryotic K^+ channels (but see Wrisch & Grissmer, 2000 for some exceptions), it is less clear that the conformation of the crystallized KcsA channel reflects the structure of the open pore of voltage-gated K^+ channels. The bundle crossing of the inner helices in the KcsA crystal structure would appear to be too narrow to allow access of some large, pore-blocking ions. Del Camino *et al.* (2000) examined the ability of quaternary ammonium ions and an inactivation peptide to protect *Shaker* K^+ channel residues in the inner end of the pore from chemical modification. Their results suggested that the inner helices of the *Shaker* protein might exist in a bent conformation forming a large vestibule at

the inner end of the pore. A similar, large (12 Å) vestibule exists in the bacterial K^+ channel, MthK, whose crystal structure has recently been solved (Jiang *et al.* 2002).

Thus, an understanding of the interaction between permeant and blocking ions in the inner end of the pore may provide insight into functions as wide-ranging as channel gating and cardiac arrhythmias. The use of quaternary ammonium ions and their analogues should help link these more functional studies with their structural counterparts (del Camino *et al.* 2000; Zhou *et al.* 2001*b*).

In a recent study of ion interactions in the inner end of the *Shaker* pore, we found that external TEA antagonizes block by internal TEA with K^+ but not with Rb^+ as the permeant ion (Thompson & Begenisich, 2000). Other evidence suggested the existence of an ion binding site located about 5 % into the membrane electric field from the internal end of the pore that can be occupied by K^+ ions or TEA but rarely (if ever) by Rb^+ ions. According to this scheme, external TEA inhibits internal TEA activity by promoting K^+ occupancy of this site by choking off K^+ efflux (Thompson & Begenisich, 2001). If this picture is correct, then the internal TEA on-rate will be reduced as internal K^+ ions fill the K^+/TEA binding site. Unfortunately, internal TEA binding kinetics are too fast (in wild-type channels) to be useful to test this hypothesis so in the study reported here we used the quaternary ammonium analogue, tetrabutyl antimony (TBSb), a compound that is sufficiently electron dense to have been observed to occupy the cavity site in KcsA. TBSb has K^+ channel blocking properties analogous to those of tetrabutyl ammonium (TBA), and kinetics slow enough to be reliably measured (Zhou *et al.* 2001*b*). We found that external TEA protected *Shaker* K^+ channels from block by internal TBSb in a manner that depended on the internal K^+ concentration. The protection from internal TBSb block was considerably larger than that from block by internal TEA. Consistent with the picture presented for the interaction between external TEA and internal TEA, the TBSb on-rate was an inverse function of the internal K^+ concentration. Surprisingly, we found significant differences between external TEA-mediated protection from block by internal TBSb and internal TEA; in particular, the protection from TBSb block occurred even when K^+ ions were replaced by Rb^+. Thus, we are forced to consider that TEA may bind at a different location than TBSb, perhaps more toward the inner end of the pore than the cavity site. Consistent with this idea, we found that internal Cs^+ ions competed with TBSb but not with TEA. These results help to define the relative location and affinities of ion binding sites in the inner end of the pore in *Shaker* K^+ channels.

METHODS

K^+ channel constructs

The experiments reported here were carried out on the inactivation-deletion version of *Shaker* B, ShB Δ6–46 (Hoshi *et al.* 1990). The T441S mutation was introduced into the ShB Δ6–46 clone using a two-step polymerase chain reaction protocol and the resulting mutant clone was analysed by DNA sequencing.

Oocyte isolation and microinjection

Frog (*Xenopus laevis*) maintenance, oocyte isolation and RNA injection used standard methods (Goldin, 1992), which have previously been described in detail (Thompson & Begenisich, 2000, 2001). The procedures for animal handling, maintenance and surgery were approved by the University of Rochester Committee on Animal Resourses. Frogs were anaesthetized with 0.2 % tricaine (Sigma) and ovarian lobes were removed. The frogs were then humanely killed. Isolated ovarian lobes were defolliculated by incubation for 60–90 min with 2 mg ml^{-1} of collagenase Type IA (Sigma-Aldrich).

Electrophysiological recordings

K^+ channel currents were recorded 1–5 days after RNA injection. Electrophysiological recordings were done at room temperature (20–22 °C) with excised inside-out or outside-out macropatches using an Axopatch 1-D amplifier (Axon Instruments, Foster City, CA, USA). Patch pipettes had tip diameters of approximately 3–6 μm constructed from Corning 7052 (Garner Glass Co, Claremont, CA, USA) or GC-150 glass (Warner Instruments Inc., Hamden, CT, USA). The measured junction potentials for the solutions used were all within 4 mV of one another and so no correction for these was applied. The holding potential was −70 mV in most cases; however, we used a holding potential of −90 mV with some experiments, especially those with 20 mM internal K^+, in order to minimize the amount of slow inactivation (Baukrowitz & Yellen 1995, 1996*b*). Data acquisition was performed using a 12 bit analog/digital converter controlled by a personal computer. Current records were filtered at 5 kHz.

The standard external solution contained (mM): 5 KCl, 135 *N*-methyl-D-glucamine (NMDG) chloride, 2 $CaCl_2$, 2 $MgCl_2$, 10 Hepes (pH adjusted to 7.2 with NMDG). Experiments with external TEA used 100 mM prepared by equimolar replacement of NMDG. The standard internal solution consisted of (mM): 110 KCl, 25 KOH, 10 EGTA, 10 Hepes (pH adjusted to 7.2 with HCl). NMDG replaced K^+ in solutions used for experiments with reduced K^+ content. In some experiments Rb^+ completely replaced the K^+ in these solutions. For experiments with internal Cs^+ we used a 20 mM internal K^+ solution (with NMDG as the replacement cation); Cs^+ was added at the expense of NMDG.

We used three types of internal blocking molecules in this study: TEA, tetrabutyl ammonium (TBA) and tetrabutyl antimony (TBSb) all from Aldrich Chemical Co. (Milwaukee, WI, USA). Depolarizing pulses were applied at a very low rate (one every 15 s in order to avoid induction of C-type inactivation with TBA and TBSb (Baukrowitz & Yellen 1995, 1996*a*).

Data analysis

The apparent K_d values for *Shaker* channel inhibition by the various internal blocking ions were obtained from measurements of block by different blocker concentrations as in Fig. 1. The K_d values were obtained by fitting these dose–response relations with the standard single-component Langmuir equation.

We obtained apparent on- and off-rates for inhibition by the internal blocking ions from the steady-state level and the time constant (τ) for block (see Fig. 3):

$$k_{on} = F_B/\tau \quad \text{and} \quad k_{off} = (1 - F_B)/\tau,$$

where F_B is the steady-state fraction of current blocked. As illustrated in Fig. 3, we obtained estimates of the block time constant, τ, by fitting a single exponential to the current decline in the presence of the blocking ion. No change in the estimated τ values was obtained by fitting two exponentials to the last half of the activation phase plus the inhibition time course.

Exponential fits were carried out using our implementation of the Simplex algorithmn (Caceci & Cacheris, 1984); fits of all other equations to the data were carried out using the Levenberg-Marquardt algorithm as implemented in Origin 6.1 (OriginLab Corp., Northampton, MA, USA). Error limits for the fitted parameters are the estimated errors from the fitting routine.

RESULTS

External TEA protects from block by internal TBSb

Figure 1 shows that external TEA protects *Shaker* K+ channels from block by internal TBSb. The pair of currents in the left inset in Fig. 1*A* illustrates channel block by 5 μM internal TBSb. In 135 mM internal K+, this concentration of TBSb blocked approximately 50 % of the current. Addition of external TEA substantially reduced the amount of block by this concentration of TBSb (Fig. 1*A*, right inset showing pair of current records). The main part of Fig. 1*A* shows the concentration dependence of block by internal TBSb in the absence (□) and presence (●) of external TEA. Both relations are well fitted by a standard Langmuir relation and external TEA increased the apparent K_d value for internal TBSb block by 7-fold from 4.4 ± 0.34 to 30 ± 1.9 μM.

The protection from internal TBSb block afforded by external TEA depended on the internal K+ concentration. This is illustrated in Fig. 1*B*. The insets show block of raw currents by 5 μM internal TBSb with 20 mM internal K+ in the absence (left) and presence (right) of external TEA. The main part of Fig. 1*B* shows that external TEA increased the apparent K_d for block by internal TBSb by only about a factor of two (from 6.1 ± 0.52 to 12 ± 0.85 μM).

We obtained similar data in solutions with other concentrations of internal K+. These are summarized in Fig. 2. The data represented by open squares in Fig. 2*A* show that, in the absence of external TEA, there was little, if any, affect of internal K+ concentration on the apparent K_d for block by internal TBSb. In the presence of external TEA (●), the apparent K_d initially increased quite steeply with internal K+ concentration and then appeared to reach an approximately constant level. The steepness of the relationship between the apparent K_d and internal K+ concentration is highlighted by the dotted line that represents a saturating hyperbola with a Hill coefficient of 2, suggesting that two or more K+ ions may be involved in the mechanism underlying this observation.

External TEA protected the channel from internal TBA block in a manner quite similar to the protection from TBSb block. Included in Fig. 2*A* are measurements of block by TBA in the absence (◇) and presence (◆) of external TEA. External TEA increased the apparent K_d for block by internal TBA by an amount almost identical to the protection from TBSb block. Thus, replacing the nitrogen atom with the more electron dense antimony has little or no effect on how these quaternary compounds interact with inner pore of K+ channels (Zhou *et al.* 2001*b*).

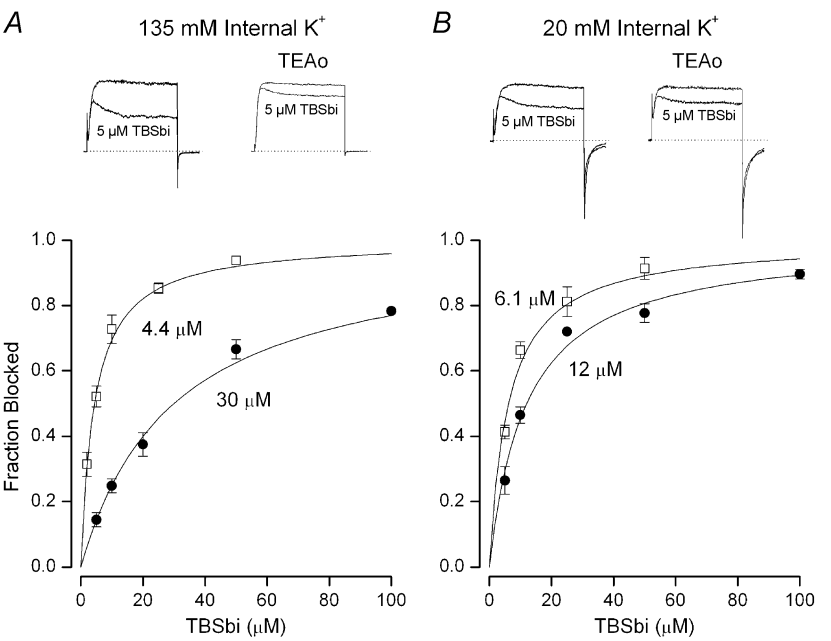

Figure 1. External TEA protection from block by internal TBSb depends on internal K+

A, fraction of current (at 0 mV) blocked by internal TBSb in 135 mM internal K+ in the absence (□) and presence (●) of 100 mM external TEA. Mean values with S.E.M. limits from 4–6 measurements at each TBSb concentration in the absence and 3–7 measurements at each TBSb concentration in the presence of external TEA. *B*, similar data obtained in 20 mM internal K+; S.E.M. limits omitted if smaller than the symbol. Insets: raw current records from 80 ms voltage clamp steps from −70 to 0 mV in the absence (left) and presence (right) of 100 mM external TEA. Lower current record in each panel obtained with 5 μM internal TBSb. Apparent K_d values for internal TBSb block are indicated and described in text.

As described in Methods, we varied the internal K^+ concentration by equimolar replacement with NMDG. In order to test for a possible involvement of NMDG in the results of Fig. 2*A*, we also measured block by internal TBSb in a solution with 75 mM K^+ and no NMDG (osmotic balance maintained with glucose). The apparent K_d for TBSbi block in the absence (△) and presence of external TEA (▲) was not different from that with NMDG.

The relationship between block by internal TBSb in the presence of external TEA is quantitatively and qualitatively quite different from the results with internal TEA block (Thompson & Begenisich, 2001) illustrated in Fig. 2*B*. Quantitatively, external TEA produced only about a 3-fold increase in the apparent K_d for internal TEA block in 135 mM internal K^+. This quantitative difference is emphasized by comparing these data on the same scales (Fig. 2*A* and *B*). Not only is there a large quantitative difference between block by internal TEA and TBSb in the presence of external TEA but there is no sign of the saturation of the apparent K_d for internal TEA as there is for the TBSbi data.

The continuous line in Fig. 2*B* is the prediction of a simple model for external TEA protection from block by internal TEA. In this model the protection depends on the concentration of internal K^+: TEA and internal K^+ ions compete for occupancy of a site near the inner end of the pore; the inhibition of K^+ efflux by external TEA promotes occupancy of the site by internal K^+ ions and so block by internal TEA is reduced. The block of K^+ efflux by external TEA puts the K^+ channel pore in true equilibrium with the contents of the internal solution. Thus, this model predicts (Thompson & Begenisich, 2001) that, in the presence of a high concentration of external TEA, the apparent affinity for block by internal TEA (K_i^{app}) will be a linear function of the internal K^+ concentration:

$$K_i^{app} = K_i(1 + ([K^+]_i/K_K)),$$

where K_i and K_K are the intrinsic site affinities for TEA and K^+ ions, respectively. The fit of this relation to the internal TEA data of Fig. 2*B* (●) indicates the site has an affinity of 68 ± 14 mM for K^+ ions and 0.49 ±0.06 mM for internal TEA (Thompson & Begenisich, 2001). Thus, the interaction between internal TEA and K^+ ions in the *Shaker* pore is a simple competitive one. The interaction between TBSb and K^+ ions is much more complex than the interaction between TEA and K^+ ions as illustrated by the complex relationship between TBSb block and internal K^+

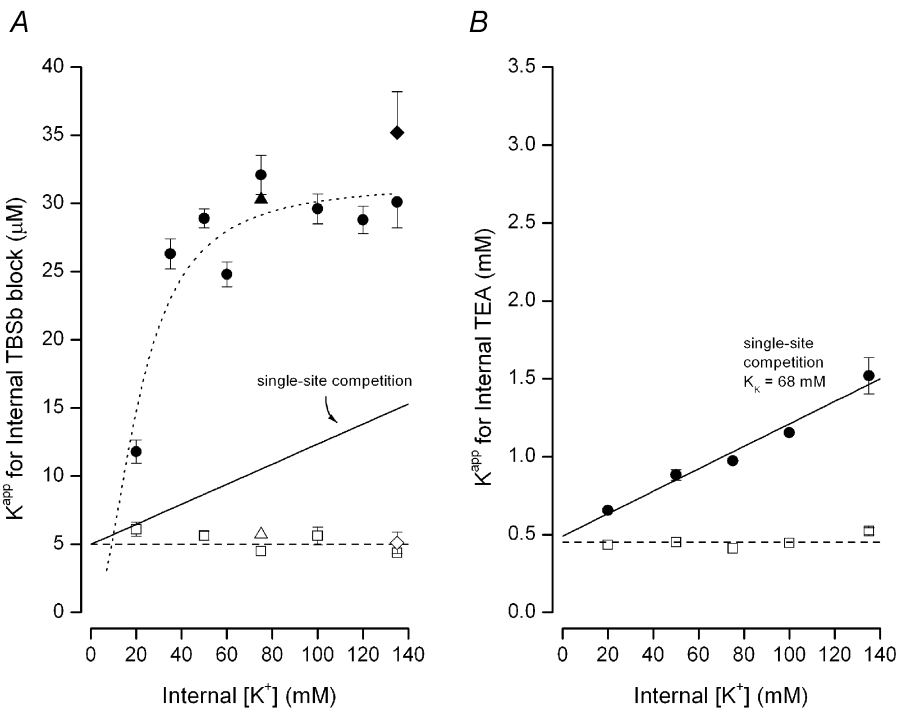

Figure 2. Internal K^+ sensitivity of apparent K_d for block by internal ions

A, apparent K_d for block by internal TBSb (obtained as in Fig. 1) in the absence (□) and presence (●) of 100 mM external TEA. As described in text, the triangles represents data (with 75 mM K^+) obtained with NMDG replaced by glucose (see Methods) in the absence (△) and presence (▲) of 100 mM external TEA. Diamonds represent apparent K_d value of TBA block obtained in the absence (◇) and presence (◆) of 100 mM external TEA. Dashed line at 5 μM shown for reference purposes. The other lines are described in the text. *B*, apparent K_d for block by internal TEA in the absence (□) and presence (●) of 100 mM external TEA; data from Thompson & Begenisich (2001). Dashed line at 0.45 mM shown for reference purposes. The continuous line is described in text. Error estimates omitted if smaller than symbols.

(●, Fig. 2*A*). This point is emphasized by the continuous line in Fig. 2*A* which is the prediction of the simple competitive model with 68 mM for the affinity of the site for K^+ ions and an intrinsic affinity for internal TBSb of 5 μM. Clearly, this model provides a poor description of the interaction of K^+ ions and TBSb, underscoring the complexity of the interaction between these ions in the pore of *Shaker* channels.

Information on the mechanism of internal K^+ and TBSb interaction in the pore can come from knowledge of the TBSb on- and off-rates. Fortunately, like its ammonium counterpart, tetrabutyl ammonium, the kinetics of block by TBSb are slow enough to resolve in a standard voltage clamp experiment (Zhou *et al.* 2001*b*), as can be seen in the raw currents in the insets of Fig. 1. Similar data obtained in 135 mM internal K^+ are illustrated in the inset of Fig. 3. The smaller current shows the time course of block by 25 μM TBSb which was well fit by a single exponential time function (thin line). As described in Methods, the time constant and steady level of block allow determination of the individual TBSb on- and off-rates. Mean values of the internal TBSb on- and off-rates in 135 mM internal K^+ are shown in the main part of Fig. 3. The on-rate appeared to be a linear function of the internal TBSb concentration and the off-rate was independent of TBSb concentration – consistent with simple bimolecular reaction kinetics.

We determined the TBSbi on- and off-rates using the method illustrated in Fig. 3 with solutions of different concentrations of internal K^+ and in both the absence and presence of external TEA. The insets above the main parts of Fig. 4*A* and *B* provide additional examples of this method of determining the on- and off-rates, respectively, in 20 mM (▲) and 135 mM internal K^+ (▽). In the absence of external TEA, both the on- and off-rates (□ in Fig. 4*A* and *B*, respectively) appeared to be fairly independent of internal K^+ except at the lowest concentration used. In contrast to the minimal effect of internal K^+ ions on the TBSb kinetics in the absence of external TEA, the TBSb on-rate was substantially reduced by increased concentrations of internal K^+ ions when the pore was blocked by external TEA (●, Fig. 4*A*).

The decline of the apparent TBSb on-rate with internal K^+ concentration in the presence of external TEA is precisely the behaviour expected if internal K^+ and TBSb ions competed for a single site whose K^+ occupancy was enhanced when external TEA inhibited K^+ efflux from the pore. This mechanism is sufficient to account for the ability of external TEA to protect from block by internal TBSb in a K^+ concentration-dependent manner: (1) raising the internal K^+ concentration increases occupancy of the site by K^+ ions; (2) since TBSb ions cannot occupy the site until it is empty of K^+ ions, the apparent on-rate would be reduced as the internal K^+ concentration is increased.

Thus, much of the ability of external TEA to protect from internal TBSb block can be accounted for by the decrease in on-rate as a function of the internal K^+ concentration. However, as can be seen in Fig. 4*B*, there were two additional, unexpected effects that reflect the interaction between internal TBSb and K^+ ions: (1) blocking the pore with external TEA produced an increase in the apparent TBSb off-rate, even at the lowest internal K^+ concentration and (2) the off-rate in the presence of external TEA (●) declined with increased concentration of internal K^+.

The increase in the apparent off-rate of TBSb induced by external TEA could occur if there were a K^+ binding site located more toward the external entrance of the pore than the TBSb site. The increase in the TBSb off-rate could be the result of an electrostatic repulsion from a K^+ ion occupying this 'enhancement' site. This K^+ binding site would appear to have a rather high intrinsic affinity as the increase in the TBSb off-rate occurred even at the lowest internal K^+ concentrations used.

The reduction of the off-rate at increased internal K^+ concentration is consistent with the presence of a binding site for K^+ ions in the pore located more toward the internal solution than the TBSbi site: the occupancy of this site by K^+ ions would 'lock' TBSb in the pore. The ability of K^+ ions to both 'lock-in' TBSb and to 'enhance' the TBSb off-rate is reminiscent of analogous effects of internal K^+ ion on Ba^{2+} block of maxi-K channels (Neyton & Miller, 1998*a*,*b*).

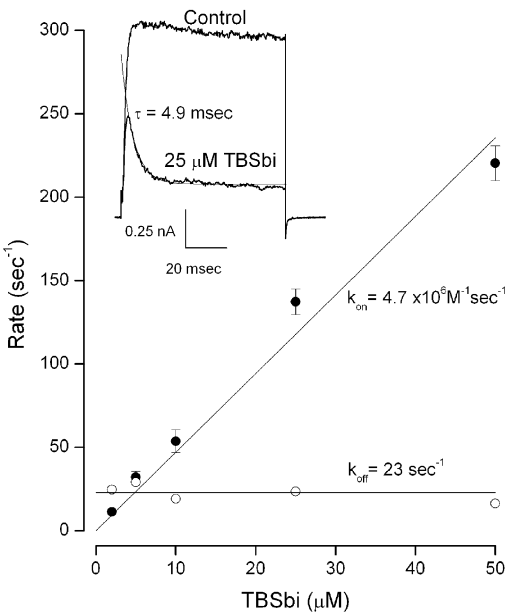

Figure 3. On- (●) and off- (○) rates for TBSb block in 135 mM internal K^+

Mean values with S.E.M. limits from 4–7 measurements at each TBSb concentration. Lines: linear fits with k_{on} and k_{off} values of $(4.7 \pm 0.15) \times 10^6$ M^{-1} s^{-1} and 23 ± 1.3 s^{-1}. Inset: raw data records in the absence (Control) and presence of 25 μM internal TBSb. Thin line: exponential fit to TBSb data with a time constant of 4.9 ms.

The steepness of the relationship between the apparent TBSbi affinity and internal K^+ (●, Fig. 2*A*) and the different internal K^+ sensitivities of the TBSb on-rate (Fig. 4*A*, ●) and off-rate (Fig. 4*B*, ●) suggest the presence of two K^+ ion binding sites that interfere with occupancy of the pore by TBSb, in addition to the third enhancement K^+ site. Thus, temporarily ignoring the enhancement site, the inner part of the pore can be considered to contain two sequential K^+ ion binding sites. We consider that TBSb ions bind only to a single site since the TBSb dose–response relations (Fig. 1) are fitted well by a single population of receptors with a 1:1 stoichiometry.

Thus, the state diagram for the inner end of the pore (when blocked by external TEA ions) can be represented as:

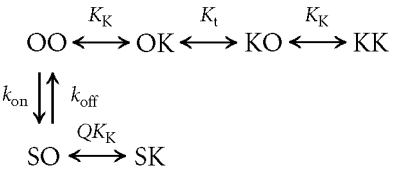

Scheme 1

O represents an empty site, and K and S represent K^+ and TBSb ions, respectively. The cytoplasmic end of the pore is on the right in this scheme. Since the pore is blocked by external TEA (not illustrated), these sites are in true thermodynamic equilibrium with the ions in the internal solution. K_K represents the intrinsic affinity of the innermost site for K^+ and K_t represents the K^+ equilibrium between the two sites. k_{on} and k_{off} are the intrinsic on- and off-rates for TBSb binding to its site. The Q term allows for the possible difficulty of K^+ ions binding behind the charged and bulky TBSb molecule.

Both sites in Scheme 1 must be empty for TBSb to bind to its site and so the apparent on-rate for TBSb block will be a function of both K_K and K_t:

$$k_{on}^{app} = \frac{k_{on}}{1 + \frac{[K^+]_i}{K_K}\left(1 + \frac{1}{K_t}\right) + \left(\frac{[K^+]_i}{K_K}\right)^2\left(\frac{1}{K_t}\right)}. \quad (1)$$

Our previous work (Thompson & Begenisich, 2001; see Fig. 2*B*) showed that, when the pore is blocked by external TEA, internal K^+ ions compete with internal TEA for a

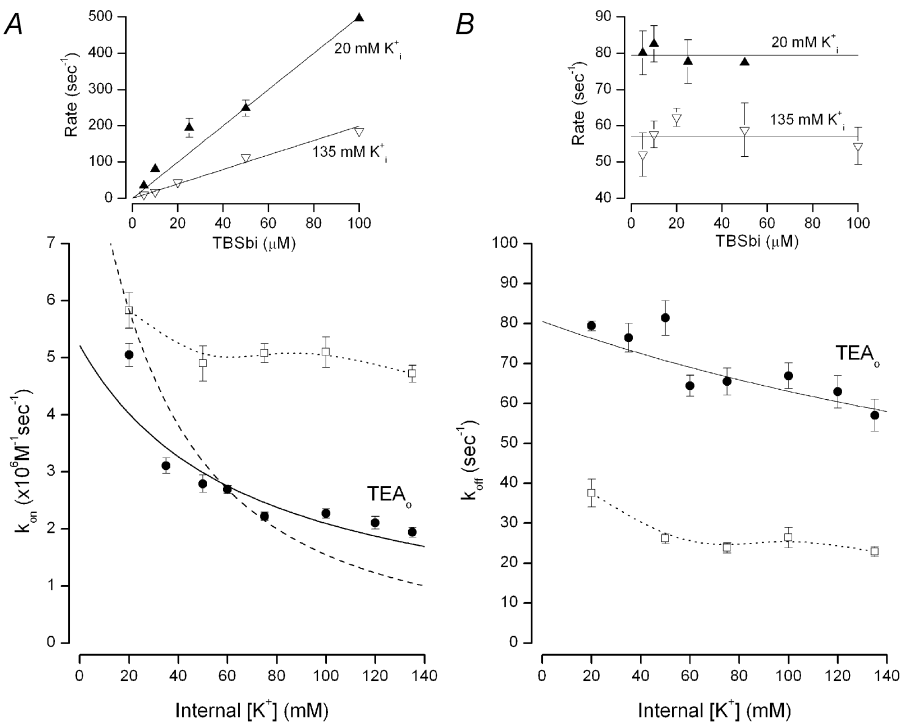

Figure 4. Internal K^+ dependence of on- and off-rates for TBSb block

A, the internal K^+ dependence of the on-rate for internal TBSb block in the absence (□) and presence (●) of 100 mM external TEA. Rates determined as illustrated in Fig. 3. Continuous line and dashed line as described in the text. The dotted line connects the symbols representing the data obtained in the absence of external TEA and has no mechanistic meaning. *B*, the internal K^+ dependence of the internal TBSb off-rate obtained in the absence (□) and presence (●) of 100 mM external TEA. Continuous line as described in the text. The dotted line connects the symbols representing the data obtained in the absence of external TEA and has no mechanistic meaning. Insets: examples of determinations of on-rate (left) and off-rate (right) in 20 mM (▲) and 135 mM (▽) internal K^+. The very large block by 100 μM TBSb in 20 mM internal K^+ makes computation of the off-rate unreliable (see eqations in Methods) and so is not included. Error bars not illustrated if smaller than symbol.

single ion binding site. In Scheme 1 this is the K^+ site closer to the inner end of the pore. From this competition between internal TEA and K^+ we estimated that K^+ ions bind to this site with an affinity near 68 mM. We (Thompson & Begenisich, 2001) also estimated the affinity of this site by another method, which yielded a value of 64 ± 14 mM for the affinity of this site for K^+ ions (Thompson & Begenisich, 2001). Thus, two independent methods show that internal K^+ ions may bind to the inner most site in Scheme 1 with an affinity, K_K, near 65 mM.

If the equilibrium constant between the two K^+ sites in Scheme I, K_t, is near or less than unity, the quadratic term in the internal K^+ concentration of eqn (1) will be significant – predicting a very steep dependence of the apparent k_{on} on internal K^+ concentration. This is illustrated in Fig. 4*A* by the dashed line which is a fit of eqn (1) to the data, with a K_t value of 1 and the K_K value set at the previously determined value of 65 mM. This line provides a poor fit to the data; in particular it predicts a much steeper dependence on internal K^+ than seen in the data.

If, as suggested by the preceding analysis, the equilibrium constant K_t is much larger than unity, then intracellular K^+ ions will still inhibit the ability of TBSb to reach its binding site but not by directly competing with TBSb for the deeper site. Rather, K^+ ion occupancy of the site closer to the inner end of the pore will prevent access of TBSb to its site deeper in the pore. Under these conditions, eqn (1) reduces to the simpler form:

$$k_{on}^{app} = \frac{k_{on}}{1 + \frac{[K^+]_i}{K_K}}.$$

The continuous line in Fig. 4*A* represents the fit of this equation to the apparent on-rate data obtained in the presence of external TEA (●) with an intrinsic k_{on} value of $(5.2 \pm 0.98) \times 10^6$ M^{-1} s^{-1} and a K_K value of 67 ± 7.9 mM, consistent with the 65 mM estimates of this parameter described above. The model prediction deviates from the data at the lowest internal K^+ concentrations – perhaps owing to some contribution of K^+ occupancy of the deeper site or the enhancement site described above. In any case, Scheme 1 with a large value for the equilibrium constant, K_t, and an affinity of about 65 mM for the innermost K^+ site, captures the essence of how the TBSbi on-rate is influenced by internal K^+ ions.

Another prediction of Scheme 1 is that TBSb will be locked in by K^+ ion occupancy of the innermost site, with an apparent off-rate for TBSb given by:

$$k_{off}^{app} = \frac{k_{off}}{1 + \frac{[K^+]_i}{QK_K}}. \quad (2)$$

We fitted eqn (2) to the off-rate data (●) of Fig. 4*B* (continuous line). In the context of this model, the decrease in the apparent off-rate with increased internal K^+ is the result of the binding of K^+ ions behind TBSb. The internal K^+ sensitivity of this inhibition is rather less than expected from a K^+ site with an affinity of 65 mM, as if the binding of K^+ to this site was inhibited by the presence of the bulky (and charged) TBSb ion. The fit of eqn (2) to the data suggests that TBSb reduced the apparent affinity of this K^+ site by a factor (Q) of about 5.4.

TBSbi block in Rb^+ solutions

The ability of external TEA to inhibit block by internal TEA seen with 135 mM intracellular K^+ is entirely absent if

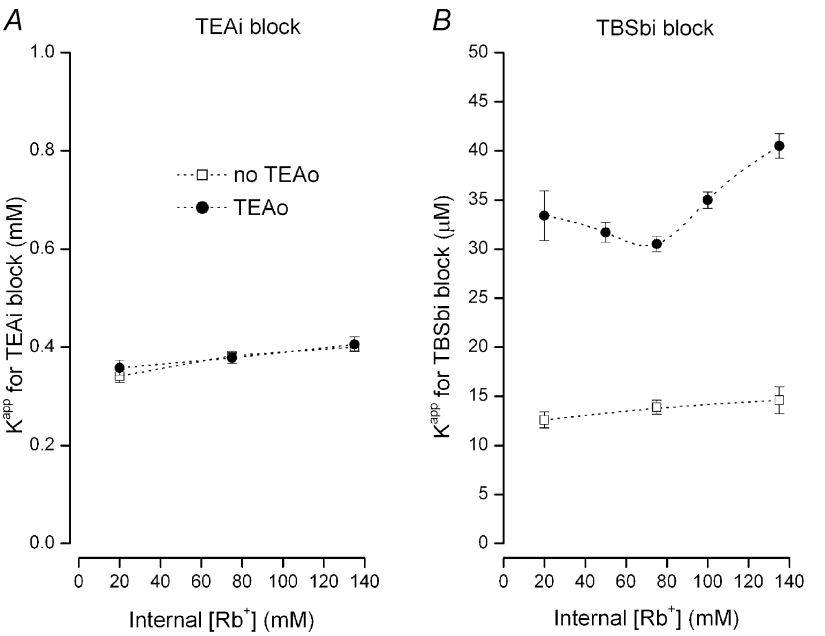

Figure 5. Internal block by TEA and TBSb in Rb^+ solutions

A, apparent K_d for block by internal TEA in the absence (□) and presence (●) of 100 mM external TEA. *B*, apparent K_d for block by internal TBSb in the absence (□) and presence (●) of 100 mM external TEA. Dotted lines connect data points and have no physical significance.

Rb^+ replaces K^+ in this solution (Thompson & Begenisich, 2000). We extended this analysis to lower internal Rb^+ concentrations (Fig. 5*A*) with the same result: internal Rb^+ ions had no effect on internal TEA block, with or without external TEA. These results, as we previously suggested (Thompson & Begenisich, 2001), show that the site for which internal K^+ and TEA ions compete has a negligible affinity for Rb^+ ions.

The data in Fig. 5*B* illustrates block of *Shaker* K^+ channels by TBSb in Rb^+ solutions. As for block by internal TEA, there was essentially no effect of internal Rb^+ on internal TBSb block in the absence of external TEA (□, Fig. 5*B*). However, in sharp contrast to the results with internal TEA, external TEA is able to protect the channel from block by internal TBSb in Rb^+ solutions (●, Fig. 5*B*). External TEA reduced the apparent affinity of internal TBSb by about 2.5- to 3-fold for internal Rb^+ concentrations of 20 to 140 mM.

In order to probe the mechanism of TBSb block in Rb^+ solutions, we determined the on- and off-rates for TBSbi block and the results are illustrated in Fig. 6. Changes in the concentration of internal Rb^+ had little effect on the on- or off-rates in the absence of external TEA (□, Fig. 6*A* and *B*). However, there was an approximate 2-fold increase in the TBSbi off-rate when TEA blocked the external end of the pore (compare □ and ● in Fig. 6*B*), suggesting that the enhancement site can be occupied by Rb^+ as well as K^+ ions – even at the lowest Rb^+ concentration used (20 mM). The addition of external TEA produced a small (25–30 %) reduction in the on-rate that was essentially independent of the Rb^+ concentration. However, neither the on- nor off-rate for internal TBSb block in the presence of external TEA changed substantially with increased Rb^+, suggesting that neither the TBSb site nor the lock-in site has an appreciable affinity for Rb^+. The factor-of-two increase in the TBSbi off-rate and the 25–30 % decrease in the on-rate would account for most of the 2.5- to 3-fold increase in the apparent K_d seen in Fig. 5*B*.

Different binding sites for internal TEA and TBSb?

The results presented here have illustrated several differences between how internal TEA and TBSb blocked the pore of *Shaker* K^+ channels. In the presence of external TEA, the internal K^+ concentration dependence of the apparent inhibition constant for TBSb block (Fig. 2*A*) was considerably steeper than that for internal TEA (Fig. 2*B*), reached a much larger value, and saturated at K^+ concentrations above 75 mM. In addition, internal Rb^+ ions had no effect on block by internal TEA (Fig. 5*A*) but did affect block by internal TBSb (Fig. 5*B*). Thus, there appears to be something quite different about how TEA and TBSb interact with permeant ions in the pore in these

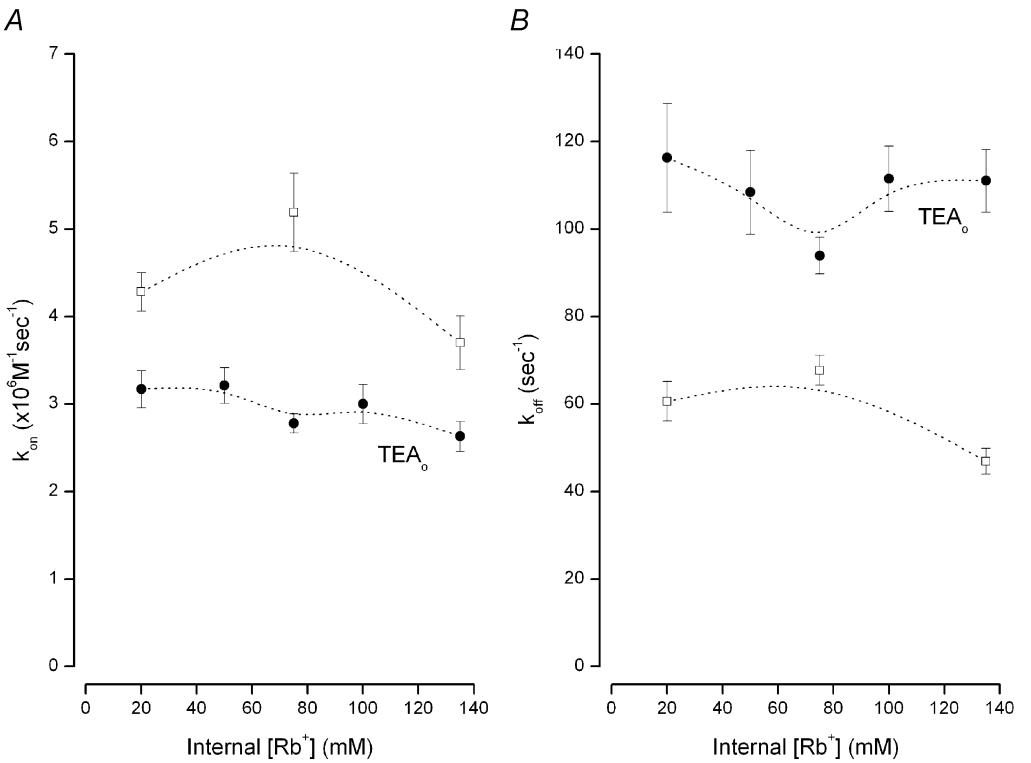

Figure 6. Internal Rb^+ dependence of on- and off-rates for TBSb block

A, the internal Rb^+ dependence of the on-rate for internal TBSb block in the absence (□) and presence (●) of 100 mM external TEA. *B*, the internal Rb^+ dependence of the internal TBSb off-rate obtained in the absence (□) and presence (●) of 100 mM external TEA. Dotted lines connect data points and have no physical significance.

channels. Since block by external TEA causes the inner end of the pore to be in true thermodynamic equilibrium with the internal solution, the possible mechanisms for the origin of these differences are limited. The simplest possibility is that internal TEA and TBSb do not bind to identical sites. Since TBSb has been localised to the cavity in KcsA, and TEA and other quaternary ammonium compounds are also considered to bind in the cavity, this is a rather unattractive suggestion. Thus, we sought an additional test of this idea.

Cs^+ ions occupy the cavity site in KcsA channels (Doyle *et al.* 1998) and block voltage-gated K^+ channels in a voltage-dependent manner when added to the intracellular solution (e.g. Bezanilla & Armstrong, 1972). Therefore, Cs^+ ions should compete with any ion that also occupies the pore cavity. If TBSb and TEA share a common binding site in the pore cavity, then intracellular Cs^+ ions should interfere equally with block by TBSb and TEA. Figure 7 presents the results of a test of the competition of internal Cs^+ ions with TBSb and with TEA.

As illustrated in Fig. 7*A*, internal Cs^+ strongly interfered with block by TBSbi but had only a modest effect on block by TEA. The apparent K_d for block by internal TBSb increased significantly as the concentration of internal Cs^+ was increased (■, Fig. 7*A*). A concentration of internal Cs^+ of 45 mM increased the apparent K_d for TBSb block by more than 3-fold. Block by internal TEA was much less affected by internal Cs^+ (○, Fig. 7*A*): the apparent K_d for internal TEA block was increased only 40 % by 45 mM Cs^+. The data presented in Fig. 7*B* show that the inhibition of TBSb affinity by internal Cs^+ ions was mediated mostly through a decrease in the on-rate (■, Fig. 7*B*), with only a modest effect on the off-rate (●, Fig. 7*C*). The strong competition between Cs^+ ions and TBSb (Fig. 7*A*) is consistent with a common binding site for these two ions. The weak interaction between Cs^+ and TEA suggests that this latter ion binds at another location in the pore.

Baukrowitz & Yellen (1996*b*) found that TEA and alkyl chain triethylammonium ions differed in their ability to modulate C-type inactivation of *Shaker* K^+ channels and suggested that these ions bind to distinct (but overlapping) subsites in the inner end of the pore. The strong competition between Cs^+ ions and TBSb and the weak interaction between Cs^+ and TEA (Fig. 7*A*) suggests TEA and TBSb may, likewise, bind to distinct sites in the pore. Choi *et al.* (1993) and Baukrowitz & Yellen (1996*b*) showed that TEA and longer chain triethylammonium ions also differ in their sensitivity to mutation of an amino acid (*Shaker* location 441) near the inner end of the

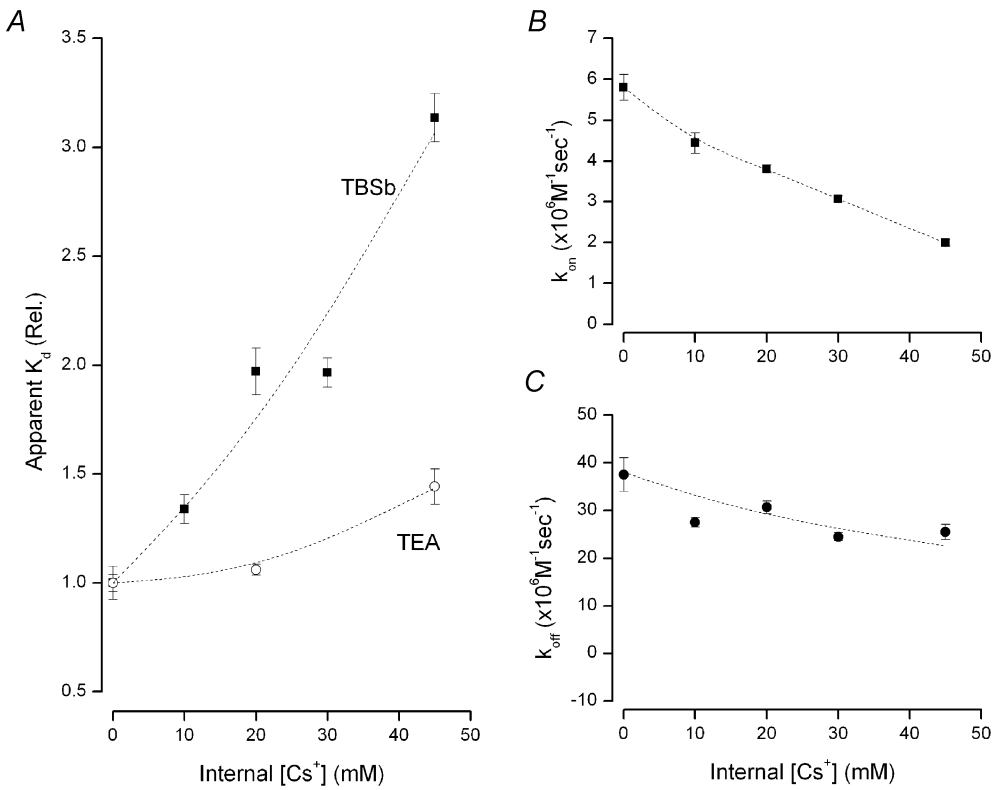

Figure 7. Competition between internal Cs^+ ions and TBSb and TEA

A, relative apparent K_d for block by TBSb (■) and TEA (○) at the indicated concentrations of internal Cs^+. *B*, on-rate for TBSb block at the indicated internal Cs^+ concentrations. *C*, off-rate for TBSb block at the indicated internal Cs^+ concentrations. $[K^+]$ in internal solution 20 mM. The lines have no physical meaning and serve only to connect the data points.

selectivity filter. The results presented in Fig. 8 show that the T441S mutation, likewise, had a differential effect on TEA and TBSb binding affinity.

The current records in the left panels of Fig. 8*A* and *B* show that the T441S mutation substantially reduced the sensitivity of *Shaker* channels to block by 5 mM internal TEA. We found that 5 mM internal TEA blocked T441S channels by an average of 49 ± 1 % ($n = 4$). Thus, this mutation increased the apparent affinity for internal TEA block to about 5 mM: 10-fold higher than wild-type channels (Thompson & Begenisich, 2001 and Fig. 2*B*), consistent with the previously reported effects of this mutation (Yellen *et al.* 1991; Choi *et al.* 1993). In contrast, the T441S mutation had little or no effect on block by internal TBSb (compare right panels of Fig. 8*A* and *B*). The average block by 5 μM TBSb of T441S channels was 54 ± 2.6 % ($n = 4$), equivalent to an apparent affinity of 4.3 μM, essentially identical with the value determined for wild-type channels (Fig. 1*A*). Thus, a mutation very near the inner end of the selectivity filter had a profound effect on TEA block but did not affect block by TBSb. As noted above, this result is similar to the findings of (Choi *et al.* 1993) comparing internal TEA with long-chain TEA derivatives and illustrates yet another significant difference between occupancy of the inner end of the pore by TEA and TEA analogues, including TBSb.

DISCUSSION

K and Rb^+ ions act differently in the pore of *Shaker* K^+ channels

Our previous results (Thompson & Begenisich, 2001) and those presented here show that K^+ and Rb^+ ions act quite differently in the pore of *Shaker* K^+ channels. (1) In the absence of external TEA, changing the permeant ion from K^+ to Rb^+ produced a 3-fold decrease in the apparent affinity for block by internal TBSb (compare data represented by open squares in Figs 2*A* and 5*B*) caused predominantly by an increase in the TBSb off-rate in Rb^+ solutions (cf. open squares in Figs 4*B* and 6*B*); TBA is similarly affected by a switch from K^+ to Rb^+ solutions (Ding & Horn, 2002). (2) In the presence of external TEA, the apparent affinity for block by internal TEA depended significantly on the internal K^+ concentration (Thompson & Begenisich, 2000; Fig. 2*B*, this paper) but was entirely insensitive to changes in Rb^+ concentration (Fig. 5*A*). (3) TBSb on- and off-rates in the presence of external TEA differed greatly in K^+ and Rb^+ solutions (compare Figs 4 and 6), accounting for the large differences in the behaviour of the apparent TBSb affinities (compare filled circles in Figs 2*A* and 5*B*). Thus, these ions either occupy different sites in the pore or occupy the same sites to substantially different degrees.

These differences between the interaction of K^+ and Rb^+ with TEA, TBA and TBSb in the inner end of the K^+ channel pore are not surprising as there are several other examples of similar differences between how K^+ and Rb^+ act in K^+ channel pores: (1) the relative conductance of Rb^+ and K^+ ions spans more than a 20-fold range in Kv2.1, *Shaker*, KcsA, Kir2.1 and maxi-K channels (Eisenman *et al.* 1986; Kirsch *et al.* 1992; Heginbotham & MacKinnon, 1993; Choe *et al.* 2000; LeMasurier *et al.* 2001); (2) the high-affinity binding site in maxi-K channels prefers Rb^+ over K^+ by about 5-fold (Neyton & Miller, 1988*a*); and (3) K^+ is 8.5 times more effective than Rb^+ at enhancing the off-rate of Ba^{2+} in the pore of maxi-K channels (Neyton & Miller, 1988*b*). Some of these differences may reflect only quantitative differences in the binding energies of these

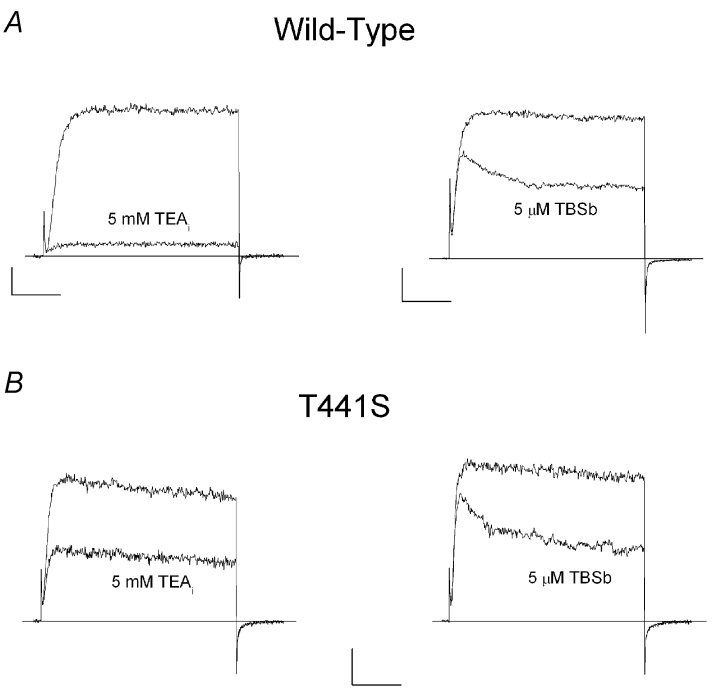

Figure 8. The T441S mutation affects block by internal TEA but not by internal TBSb

A, left, raw current records (at 0 mV) from wild-type channels in the absence (larger) and presence (smaller) of 5 mM internal TEA; right, raw current records (at 0 mV) from wild-type channels in the absence (larger) and presence (smaller) of 5 μM internal TBSb. *B*, similar records from T441S channels showing block by 5 mM internal TEA (left) and 5 μM internal TBSb (right). The holding potential was −70 mV for wild-type and −90 mV for T441S data. Horizontal and vertical calibrations: *A*, left, 10 ms and 0.1 nA; right, 20 ms and 0.2 nA. *B*, 10 ms and 0.05 nA.

ions in the pore as suggested by KcsA X-ray diffraction data and associated calculations with a simple permeation model (Morais-Cabral *et al.* 2001). However, since the selectivity filter is formed primarily of the carbonyl backbone of amino acids that are highly conserved among K^+ channels, it is not clear how the large variation in relative K^+ and Rb^+ permeation properties can be entirely accounted for by differences in their interaction with the selectivity filter. It seems reasonable to consider that additional ion binding sites may form when channels open. Certainly mutations in S6 and the S4–S5 linker alter many permeation properties (e.g. Isacoff *et al.* 1991; Lopez *et al.* 1994; Harris *et al.* 1998; Melishchuk & Armstrong, 2001) some of which have differential effects on K^+ and Rb^+ properties (e.g. Slesinger *et al.* 1993; Liu & Joho, 1998; Zei *et al.* 1999) and appear not to induce structural changes in the selectivity filter (Ding & Horn, 2002). It may be that variations in the structure of these less well-conserved regions account for some of the variation in relative K^+ and Rb^+ permeation properties among K^+ channels.

TEA and TBSb act differently in the pore of *Shaker* K^+ channels

In this study we found several fundamental differences between how internally applied TEA and TBSb interact with the inner pore of *Shaker* K^+ channels: (1) mutating amino acid 441 from a serine to a threonine greatly decreased internal TEA block but had no effect on block by TBSb (Fig. 8); (2) internal Cs^+ ions strongly interfered with TBSb but not TEA block; (3) external TEA protected the channel from block by both internal TEA and TBSb but the protection was much stronger against TBSb (Fig. 2); (4) the protection mediated by external TEA depended on internal K^+ ions for both internal blocking ions but the protection against internal TEA block was a linear function of the internal K^+ concentration and the protection against TBSb saturated at high internal K^+ (Fig. 2); (5) in the absence of external TEA, the apparent K_d for block by internal TEA was essentially unchanged when Rb^+ replaced K^+ as the permeant ion (cf. data in Figs 2*B* and 5*A*) but the apparent K_d for TBSb block increased about 3-fold when Rb^+ replaced K^+ (cf. data in Figs 2*A* and 5*B*); and (6) external TEA had no effect on the apparent affinity for internal TEA in Rb^+ solutions but produced more than a 2-fold increase in the TBSb affinity (Fig. 5). The simplest mechanism that can account for all these data is that TBSb and TEA bind at separate sites in the inner pore of *Shaker* K^+ channels.

The location of ion binding sites in the inner pore of *Shaker* K^+ channels

The results of this study, especially the determinations of the on- and off-rates for internal TBSb block, allow estimates of the affinity and relative locations of some of the ion binding sites in the inner end of the pore of *Shaker* K channels. Figure 9 illustrates the simplest arrangement of ion binding sites that is consistent with both the results of this study and with structural data from the KcsA

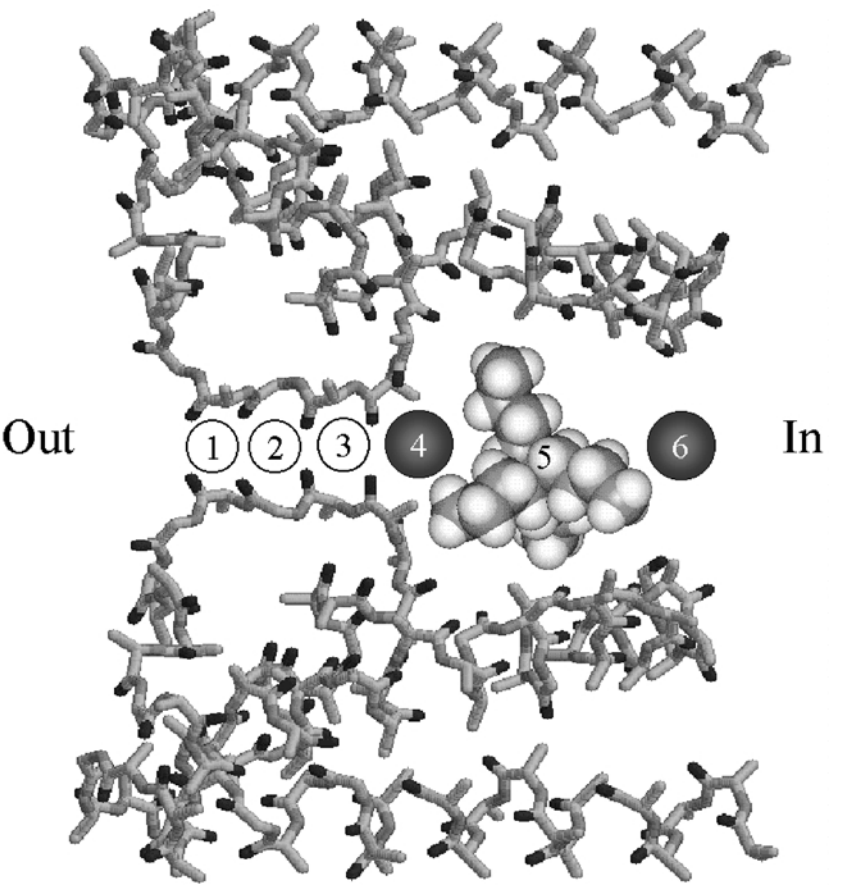

Figure 9. Relative location of ion binding sites in the inner end of the pore in *Shaker* K^+ channels

Possible sites of ion binding in *Shaker* K channels superimposed on the pore structure of the MthK channel (PDB entry 1LNQ) (Jiang *et al.* 2002). Sites labelled 1 to 6 are described in the text. Site 5 is shown occupied by a space-filling model of TBSb. This space-filling model is not intended to represent a particular structure for TBSb but only serves as an indication of its relative size. Circles occupying sites 4 and 6 represent K^+ ions and are approximately to scale with the space-filling model. 'Out' and 'In' represent the orientation of the diagram with respect to the external and cytoplasmic ends of the pore, respectively.

channel. The locations of the ion binding sites are numbered in Fig. 9 and are shown using the MthK channel (Jiang *et al.* 2002) as a structural backdrop.

Sites 1–4 follow the numbering convention of Morais-Cabral *et al.* (2001) and are sites of K^+ and Rb^+ occupancy of the selectivity filter. Site 5 is located in the 'cavity' region and, consistent with the crystallographic data (Zhou *et al.* 2001), is the site for TBSb binding. A K^+ or Rb^+ ion bound to site 4 would 'enhance' the TBSb off-rate (Figs 4*B* and 6*B*), probably through an electrostatic repulsion mechanism. Since K^+ ions inhibited the TBSb off-rate (Fig. 4*B*), we include site 6 as a K^+-selective 'lock-in' site. Since TBSb and TEA appear to bind at different locations and since TEA and K^+ ions compete for binding (Thompson & Begenisich, 2001), we consider site 6 as the TEA binding site.

Our findings of separate sites that accelerate TBSb off-rate and inhibit TBSb off-rate are reminiscent of the 'enhancement' and 'lock-in' sites associated with Ba^{2+} block of maxi-K channels (Neyton & Miller, 1989*a*,*b*). However, the sites that affect Ba^{2+} block are different from those that affect TBSb block. According to the X-ray crystallographic data from the KcsA channel (Jiang & MacKinnon, 2000), Ba^{2+} binds at site 4. Thus, occupancy of site 3 by a permeant ion Ba^{2+} would enhance the Ba^{2+} off-rate and permeant ion occupancy of the cavity location (site 5) would inhibit the Ba^{2+} off-rate.

The affinity of ion binding sites in the inner pore of *Shaker* K^+ channels

The permeant ion effects on TBSb and TEA block allow estimates of the affinity of some of the ion binding sites in the inner pore of *Shaker* K channels. Site 4 (the TBSb enhancement site) appears to have a reasonably high affinity for the permeant ions, Rb^+ and K^+, perhaps in the millimolar range. Such an affinity would account for the fact that the addition of external TEA increased the TBSb off-rate even at the lowest concentrations (20 mM) of Rb^+ and K^+ (Figs 4*B* and 6*B*). No additional enhancement occurred at higher concentrations of permeant ions – as if this site were saturated even at 20 mM.

The TBSbi off-rates were consistently larger with Rb^+ rather than K^+ as the permeant ion. This could be the result of a somewhat higher affinity of site 4 for Rb^+ than for K^+ ions leading to a generally greater occupancy of that site by Rb^+ and so more 'enhancement'.

In the scheme illustrated in Fig. 9, K^+ ions compete with TBSb for binding to site 5. Occupancy of either this site or site 6 by K^+ ions will reduce the TBSb on-rate (Fig. 4*A*, ●). According to the analysis described by Scheme 1 in Results, site 5 is rarely occupied by K^+ ions and site 6 has an affinity near 65 mM. This latter value is close to the affinity of the K^+ site that competes with internal TEA (Thompson & Begenisich, 2001), supporting our assignment of site 6 as the location for internal TEA block. The comparatively low sensitivity of the TBSb off-rate to internal K^+ (Fig. 4*B*, ●) reflects, in this view, the difficulty of a K^+ ion binding to site 6 while site 5 is occupied by the large, charged TBSb molecule.

Most of the effect of Rb^+ ions on TBSb block can be ascribed to the increased off-rate upon addition of external TEA (Fig. 6*B*) that, in the scheme of Fig. 9, would be due to Rb^+ occupancy of site 4, the enhancement site. The much smaller effect on the on-rate could also be ascribed to a long-range electrostatic interference from this enhancement site. The minimal effects of changes in Rb^+ concentration suggest that sites 5 and 6 are rarely occupied by Rb^+ ions. The lack of effect of Rb^+ on internal TEA block (Fig. 5*B*) is consistent with this view.

The competition between internal Cs^+ ions and TBSb and TEA (Fig. 7*A*) is also consistent with the ion binding site scheme depicted in Fig. 9. The large difference in the ability of Cs^+ to interfere with TBSb and TEA indicates that Cs^+ ions have an affinity for the cavity (site 5) in the range of 20–30 mM. This is confirmed by the effect of Cs^+ on the TBSb on-rate (Fig. 7*B*). The much smaller effect of Cs^+ on TEA block would, in this picture, be due to the TEA site (site 6) having a much lower affinity for Cs^+ ions such that there is little occupancy at concentrations less than 50 mM. The small decrease in TBSb off-rate with increased Cs^+ (Fig. 7*C*) is consistent with a reluctant ability of Cs^+ to occupy site 6 locking TBSb in the cavity.

A caveat

While the effects of intracellular K^+ ions (in the presence of external TEA) on TBSb kinetics appear to be reasonably well described by Scheme 1 (continuous lines in Figs 4*A* and *B*), it should be noted that this scheme cannot account for the saturation of the K_i^{app} for TBSb seen at high internal K^+ (Fig. 2*A*). This saturation could occur if the effect of internal K^+ ions on the TBSb on-rate approached a non-zero asymptote as the data in Fig. 4*A* may suggest. We have no satisfactory explanation for how this might occur but, in the context of the schemes described here, the inhibition of the TBSb on-rate is due to occupancy of sites 5 and 6 by K^+ ions and would be complete only when both sites were filled. Perhaps raising the internal K^+ concentration fills other sites in the pore that somehow prevent complete occupancy of these superficial sites.

Summary

Our results indicate that the functional interaction of ions with the inner end of the pore in some K^+ channels may be more complex than is suggested by the X-ray crystallographic data of the bacterial channels. We showed that there are substantial differences between the interactions of TEA and its analogues TBA and TBSb with the pore in *Shaker* channels. Occupancy of the inner pore

by Rb^+ and K^+ ions also differs considerably. It is difficult to account for all these behaviours with models in which the ions are constrained to single-file motion and that are consistent with the existing structural data. The scheme depicted in Fig. 9 is one attempt in this direction. As described above, site 4 in this scheme would correspond to the Ba^{2+} binding site revealed in the studies of Neyton & Miller (1988*a*,*b*). In this view, ions binding to either or both sites 5 and 6 would 'lock' Ba^{2+} in the pore, an assignment that suggests a large difference between ion occupancy of the inner end of the pore in *Shaker* and maxi-K channels. Neyton & Miller (1988*b*) estimated that the internal lock-in site in maxi-K channels has a rather high affinity for both K^+ and Rb^+ (7 and 9 mM, respectively). Our results suggest much lower permeant ion occupancy of this region in the pore of *Shaker* K^+ channels. Thus, additional information on the relationship between channel structure and the interaction of ions (and gating) in the inner end of the pore in K^+ channels may come from a direct comparison of internal TBSb and TEA block of maxi-K and *Shaker* channels.

REFERENCES

Armstrong CM (1969). Inactivation of the potassium conductance and related phenomena caused by quaternary ammonium ion injection in squid axons. *J Gen Physiol* **54**, 533–575.

Armstrong CM (1971). Interaction of tetraethylammonium ion derivatives with the potassium channels of giant axons. *J Gen Physiol* **58**, 413–437.

Baukrowitz T & Yellen G (1995). Modulation of K^+ current by frequency and external $[K^+]$: A tale of two inactivation mechanisms. *Neuron* **15**, 951–960.

Baukrowitz T & Yellen G (1996*a*). Use-dependent blockers and exit rate of the last ion from the multi-ion pore of a K^+ channel. *Science* **271**, 653–656.

Baukrowitz T & Yellen G (1996*b*). Two functionally different subsites for the binding of internal blockers in the pore of voltage-activated K^+ channels. *Proc Natl Acad Sci U S A* **93**, 13357–13361.

Bezanilla F & Armstrong CM (1972). Negative conductance caused by entry of sodium and cesium ions into the potassium channels of squid axons. *J Gen Physiol* **60**, 588–608.

Caceci MS & Cacheris WP (1984). Fitting curves to data. *Byte* **9**, 340–362.

Choe H, Sackin H & Palmer LG (2000). Permeation properties of inward-rectifier potassium channels and their molecular determinants. *J Gen Physiol* **115**, 391–404.

Choi KL, Aldrich RW & Yellen G (1991). Tetraethylammonium blockade distinguishes two inactivation mechanisms in voltage-activated K^+ channels. *Proc Natl Acad Sci U S A* **88**, 5092–5095.

Choi KL, Mossman C, Aubé C & Yellen G (1993). The internal quaternary ammonium receptor site of Shaker potassium channels. *Neuron* **10**, 533–541.

del Camino D, Holmgren M, Liu Y & Yellen G (2000). Blocker protection in the pore of a voltage-gated K^+ channel and its structural implications. *Nature* **403**, 321–325.

Ding S & Horn R (2002). Tail end of the S6 segment: Role in permeation in Shaker potassium channel. *J Gen Physiol* **120**, 87–97.

Doyle DA, Cabral JM, Pfuetzner RA, Kuo A, Gulbis JM, Cohen SL, Chait BT & MacKinnon R (1998). The structure of the potassium channel: molecular basis of K^+ conduction and selectivity. *Science* **280**, 69–77.

Eisenman G, Latorre R & Miller C (1986). Multi-ion conductance in the high-conductance Ca^{2+}-activated K^+ channel from skeletal muscle. *Biophys J* **50**, 1025–1034.

Goldin AL (1992). Maintenance of *Xenopus laevis* and oocyte injection. *Methods Enzymol* **207**, 266–279.

Guo D & Lu Z (2001). Kinetics of inward-rectifier K channel block by quaternary alkylammonium ions: Dimension and properties of the inner pore. *J Gen Physiol* **117**, 395–405.

Harris RE, Larsson HP & Isacoff EY (1998). A permeant ion binding site located between two gates of the Shaker K^+ channel. *Biophys J* **74**, 1808–1820.

Heginbotham L & MacKinnon R (1993). Conduction properties of the cloned Shaker K^+ channel. *Biophys J* **65**, 2089–2096.

Holmgren M, Smith PL & Yellen G (1997). Trapping of organic blockers by closing of voltage-dependent K channels: Evidence for a trap door mechanism of activation gating. *J Gen Physiol* **109**, 527–535.

Hoshi T, Zagotta WN & Aldrich RW (1990). Biophysical and molecular mechanisms of Shaker potassium channel inactivation. *Science* **250**, 533–538.

Isacoff EY, Jan YN & Jan LY (1991). Putative receptor for the cytoplasmic inactivation gate in the Shaker K^+ channel. *Nature* **353**, 86–90.

Jiang Y, Lee A, Chen J, Cadene M, Chait BT & MacKinnon R (2002). The open pore conformation of potassium channels. *Nature* **417**, 523–526.

Jiang Y & MacKinnon R (2000). The barium site in a potassium channel by x-ray crystallography. *J Gen Physiol* **115**, 269–272.

Kirsch GE, Drewe JA, Taglialatela M, Joho RH, Debiasi M, Hartmann HA & Brown AM (1992). A single nonpolar residue in the deep pore of related K^+ channels acts as a K^+:Rb^+ conductance switch. *Biophys J* **62**, 136–144.

LeMasurier M, Heginbotham L & Miller C (2001). KcsA: It's a potassium channel. *J Gen Physiol* **118**, 303–318.

Lui Y, Holmgren M, Jurman ME & Yellen G (1997). Gated access to the pore of a voltage-dependent K^+ channel. *Neuron* **19**, 175–184.

Liu Y & Joho RH (1998). A side chain in S6 influences both open-state stability and ion permeation in a voltage-gated K^+ channel. *Pflugers Arch* **435**, 654–661.

Lopez GA, Jan YN & Jan LY (1994). Evidence that the S6 segment of the Shaker voltage-gated K^+ channel comprises part of the pore. *Nature* **367**, 179–182.

Melishchuk A & Armstrong CM (2001). Mechanisms underlying slow kinetics of the OFF gating current in Shaker potassium channel. *Biophys J* **80**, 2167–2175.

Mitcheson JS, Chen J, Lin M, Culberson C & Sanguinetti MC (2000). A structural basis for drug-induced long QT syndrome. *Proc Natl Acad Sci U S A* **97**, 12329–12333.

Morais-Cabral JH, Zhou Y & MacKinnon R (2001). Energetic optimization of ion conduction rate by the K selectivity filter. *Nature* **414**, 37–42.

Neyton J & Miller C (1988*a*). Potassium blocks barium permeation through a calcium-activated potassium channel. *J Gen Physiol* **92**, 549–568.

Neyton J & Miller C (1988*b*). Discrete Ba^{2+} block as a probe of ion occupancy and pore structure in the high-conductance Ca^{2+}-activated K^+ channel. *J Gen Physiol* **92**, 569–586.

Slesinger PA, Jan YN & Jan LY. (1993). The S4-S5 loop contributes to the ion-selective pore of potassium channels. *Neuron* **11**, 739–749.

Thompson J & Begenisich T (2000). Interaction between quaternary ammonium ions in the pore of potassium channels: Evidence against an electrostatic mechanism. *J Gen Physiol* **115**, 769–782.

Thompson J & Begenisich T (2001). Affinity and location of an internal K ion binding site in Shaker K channels. *J Gen Physiol* **117**, 373–383.

Wrisch A & Grissmer S (2000). Structural differences of bacterial and mammalian K^+ channels. *J Biol Chem* **50**, 39345–39353.

Yellen G (1998). The moving parts of voltage-gated ion channels. *Q Rev Biophys* **31**, 239–295.

Yellen G, Jurman ME, Abramson T & MacKinnon R (1991). Mutations affecting internal TEA blockade identify the probable pore-forming region of a K^+ channel. *Science* **251**, 939–942.

Zei P, Ogielska EV, Hoshi T & Aldrich RW (1999). Effects on ion permeation with hydrophobic substitutions at a residue that interacts with a signature sequence amino acid. *Ann NY Acad Sci* **868**, 458–464.

Zhou Y, Morais-Cabral JH, Kaufman A & MacKinnon R (2001*a*). Chemistry of ion coordination and hydration revealed by a K^+ channel-Fab complex at 2.0 Å resolution. *Nature* **414**, 43–48.

Zhou Y, Morais-Cabral JH, Mann S & MacKinnon R (2001*b*). Potassium channel receptor site for the inactivation gate and quaternary amine inhibitors. *Nature* **411**, 657–661.

Acknowledgements

We thank Dr Robert Dirksen for critical comments on an early version of this manuscript and for many thoughtful discussions. This work was supported by grants from the National Science Foundation (IBN-9514389 and IBN-0090662).